

### Coulomb excitation of $^{180}\text{Ta}$

M. Schumann and F. Käppeler

*Forschungszentrum Karlsruhe, Institut für Kernphysik III, Postfach 3640, D-76021 Karlsruhe, Germany*

R. Böttger and H. Schölermann

*Physikalisch-Technische Bundesanstalt, Bundesallee 100, D-38116 Braunschweig, Germany*

(Received 7 April 1998)

The existence of a low energetic intermediate state (IS) in  $^{180}\text{Ta}$  which provides a coupling of the stable isomer and the radioactive ground state was investigated by means of Coulomb excitation. Natural tantalum foils were irradiated by protons with incident energies between 3.0 and 3.7 MeV, and with  $\alpha$  particles in the energy range 12–20 MeV. Subsequently, the foils were counted for the induced ground state activity of  $^{180}\text{Ta}$ . From the thick target yields an IS between 0.6 and 2.2 MeV excitation energy was inferred. The population of the IS in the stellar environment of the  $s$  process depends critically on the prevailing temperatures. Current stellar models suggest  $s$ -process temperatures below  $3.1 \times 10^8$  K which lead to a negligible population of intermediate states above 1.2 MeV. Thus, the present data do not allow stringent conclusions about the destruction of  $^{180}\text{Ta}$  under these conditions, but an  $s$  process origin seems still possible. Furthermore, the experiments support the existence of a new isomer in  $^{184}\text{Re}$ . [S0556-2813(98)01209-6]

PACS number(s): 25.70.De, 26.20.+f, 27.70.+q, 97.10.Cv

#### I. INTRODUCTION

Discovered in 1802 by Ekeberg in Sweden, the element tantalum was found to be the rarest element (0.02 relative to silicon  $\equiv 10^6$ ) containing also the rarest stable isotope in the universe,  $^{180}\text{Ta}$ . These minute traces of  $^{180}\text{Ta}$  owe their existence to a long lived isomer ( $t_{1/2} \geq 1.2 \times 10^{15}$  yr) which results from the  $\Delta K = 8$  forbiddensness of the direct transition to the 8.15 h ground state. The odd-odd nucleus  $^{180}\text{Ta}$  is therefore the only isotope occurring naturally in an isomer.

Compared to other rare odd-odd nuclei ( $^{50}\text{V}/^{51}\text{V} = 0.24\%$ ,  $^{138}\text{La}/^{139}\text{La} = 0.092\%$ ), the abundance ratio  $^{180}\text{Ta}/^{181}\text{Ta}$  is about an order of magnitude smaller reflecting the difficulty to synthesize this nucleus. Not surprisingly, the origin of this isotope is still under discussion. Among other more speculative scenarios [1–4], the nucleosynthesis may be dominated by neutron capture in the  $s$  process occurring in AGB stars [5]. In order to produce  $^{180}\text{Ta}$  in solar system

abundance, temperatures of  $T_s \approx 3 \times 10^8$  K are required. At these temperatures the question arises whether the freshly produced nuclei are destroyed in the hot stellar environment before being ejected into the interstellar medium.

An effective destruction mechanism could exist if thermally excited levels in  $^{180}\text{Ta}$  act as intermediate states (IS) for induced transitions from the isomer to the ground state, resulting in a depopulation of the stable isomer (see Fig. 1). Obviously, this depopulation depends critically on the excitation energy of the IS. For an IS located below 1 MeV excitation energy,  $^{180}\text{Ta}$  would not survive the high temperatures during the  $s$  process and sizable  $s$  contributions to the solar system abundance would not be expected.

Previously, intermediate states at 2.8 and 3.6 MeV with large integrated photoabsorption cross sections were reported by Collins *et al.* [6]. However, neither these irradiations with bremsstrahlung [6], nor nuclear spectroscopic methods [7,8] were hitherto successful in detecting lower lying IS. In this

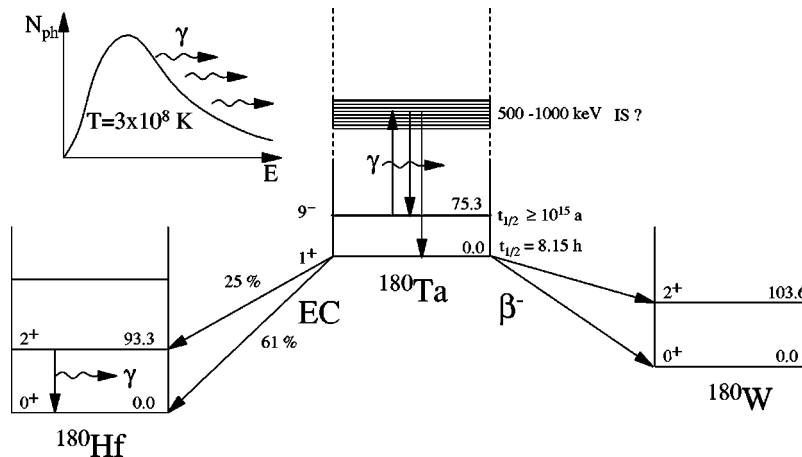


FIG. 1. Decay of  $^{180}\text{Ta}$  in the stellar environment of the  $s$  process. If thermally excited states with decay channels to isomer and ground state exist, the stable isomer will be effectively depopulated at high temperatures.

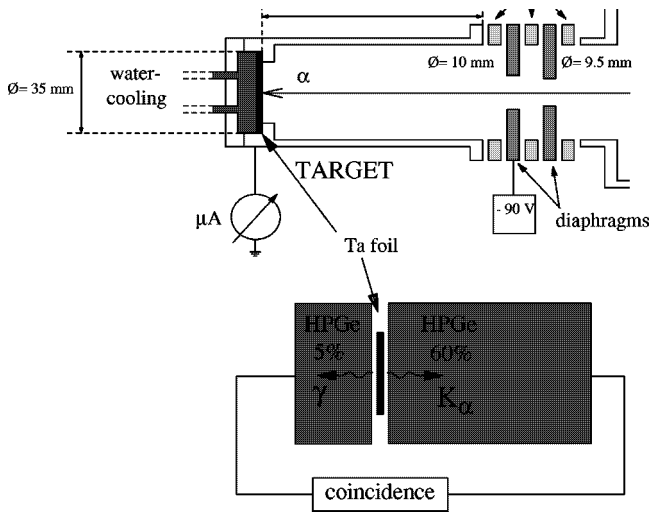


FIG. 2. Schematic sketch of the target setup and of the activity measurement for the irradiation with  $\alpha$  particles.

regard, activation by Coulomb excitation of  $^{180}\text{Ta}$  offers a promising alternative. Irradiations of natural tantalum foils with sulfur ions resulted in an increased  $^{180}\text{Ta}^g$  activity at low bombarding energies, compatible with the assumption of an IS below 1 MeV [9]. Similar results were obtained in a corresponding Coulomb excitation experiment with  $^{17,16}\text{O}$  beams [10]. Since these results were hampered by background from transfer reactions, the present work aims at an independent confirmation of the low lying IS by Coulomb excitation experiments with protons and  $\alpha$  particles.

## II. EXPERIMENTAL TECHNIQUE AND DATA ANALYSIS

The present measurements were based on the activation method. Following the irradiation of metallic tantalum foils (99.9% purity and natural composition), the depopulation of the isomer was detecting out of beam via the induced  $^{180}\text{Ta}^g$  activity.

### A. Irradiations with $\alpha$ particles

#### 1. Experimental setup and activity measurement

The irradiations were performed at the cyclotron of the Physikalisch-Technische Bundesanstalt Braunschweig (PTB). The  $\alpha$  particles had incident energies in the range 12–20 MeV, well below the Coulomb barrier ( $E_B = 24$  MeV). The water-cooled tantalum foils were part of a Faraday cup for the measurement of the integrated beam current (see Fig. 2). The foil thickness of  $d = 0.05$  to  $0.09$  mm was sufficient for stopping the  $\alpha$  particles completely. Typical beam currents of 8–17  $\mu\text{A}$  were applied since higher currents could not be tolerated due to problems with target cooling and blister formation on the surface of the foils. The measured beam current was digitized and stored in time intervals of one minute for later analysis. The beam energy was determined from the fields of two deflection magnets. According to the induced activity, irradiation times between 10 h and 12 min were chosen for different incident energies.

After the irradiations, the tantalum foils were placed in close geometry between two high purity (HP) Ge detectors of 5 and 60 % efficiency, respectively. However, in the rel-

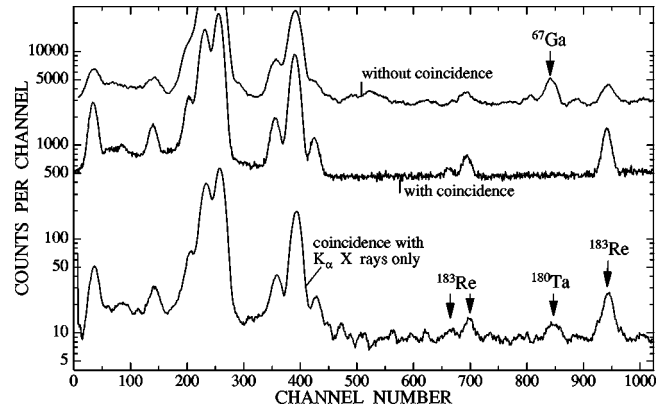


FIG. 3.  $\gamma$ -ray spectra taken with the 5% HPGe detector after the irradiation at 13.86 MeV  $\alpha$  energy. The background is reduced by almost three orders of magnitude by the coincidence with the  $K_\alpha$  x rays. This eliminates the background activity from  $^{67}\text{Ga}$  at  $E_\gamma = 93.3$  keV and allows us to isolate the few  $^{180}\text{Ta}^g$  decays ( $\leq 10$   $\text{h}^{-1}$ ). All remaining  $\gamma$  lines are due to the decay of  $^{183}\text{Re}$  and are partly marked to demonstrate the sensitivity of the measurement.

evant energy window for the  $^{180g}\text{Ta}$  decay between 50 and 100 keV, the efficiency of both detectors was practically equal, corresponding to the solid angle with respect to the activated part of the Ta foils. In fact, the thinner detector had the advantage of a significantly lower Compton background. Because of the extremely small isotopic abundance of  $^{180}\text{Ta}$ , the observed count rate was dominated by background reactions which masked the Hf x rays and the soft  $\gamma$  rays from the  $^{180}\text{Ta}^g$  decay. To reduce this background, the ground state activity was measured by the coincident detection of the 93.3 keV  $\gamma$  and the Hf  $K_\alpha$  x rays emitted in the EC decay (see Fig. 1). The efficiency of the arrangement in Fig. 2 was calibrated with standard sources ( $^{241}\text{Am}$  and  $^{109}\text{Cd}$ ) yielding a coincidence efficiency of  $\epsilon = 10.0(5)\%$  for these events. Before and after each counting period, the spectra of the two detectors were stored independently to record the count rate of other activated impurities for later pile-up corrections.

The resulting  $\gamma$ -ray spectra of the 5% HPGe detector obtained in the irradiation at 13.86 MeV are shown in Fig. 3. All spectra are given for a counting period of 12 h. The upper part illustrates the situation without coincidence requirement. Obviously, the signature of the  $^{180}\text{Ta}^g$  decay is completely masked by background activities resulting from  $\alpha$  induced reactions on  $^{181}\text{Ta}$  and on small sample impurities of 1 to 10 ppm. Especially the  $\gamma$  line at 93.3 keV from the  $^{67}\text{Ga}$  decay ( $t_{1/2} = 78.3$  h), which was produced via  $^{64}\text{Zn}(\alpha, n)$  reactions and subsequent  $\beta^+$  decay, is hindering the detection of the most intense  $\gamma$  ray from the  $^{180}\text{Ta}^g$  decay (see Table I). By the coincidence requirement (middle), this  $^{67}\text{Ga}$  activity is eliminated. However, the sensitivity is sufficiently improved only if an additional energy window is set on the 55 keV  $K_\alpha$  x rays (bottom). Compared to the measurement without coincidence requirement, the background is reduced by two to three orders of magnitude, allowing also small signals ( $\leq 10$   $\text{h}^{-1}$ ) to be detected. The half-life of the  $\gamma$  line at 93.3 keV could be verified to range between 4 and 12 h. From this information and from the unique energy signature (55 + 93.3 keV), the  $\gamma$  line at 93.3 keV was iden-

TABLE I. Photons from the  $(EC, \beta^-)$  ( $t_{1/2} = 8.152 \pm 0.006$  h [11]) decay of  $^{180}\text{Ta}^g$ .

Emitted photons	$E_\gamma$ [keV]	$I_\gamma$ [%]	Reference
Hf $L$	7.0–10.7	$23.0 \pm 3.0$	[11]
W $L$	7.4–11.4	$0.65 \pm 0.17$	[11]
Hf $K_{\alpha 2}$	54.611	$20.4 \pm 0.8$	[11]
Hf $K_{\alpha 1}$	55.790	$35.7 \pm 1.3$	[11]
W $K_{\alpha 2}$	57.981	$0.17 \pm 0.03$	[12]
W $K_{\alpha 1}$	59.318	$0.29 \pm 0.05$	[12]
Hf $K_\beta$	63.2	$15.0 \pm 0.6$	[11]
W $K_{\beta 1}$	67.155	$0.097 \pm 0.016$	[12]
W $K_{\beta 2}$	69.342	$0.025 \pm 0.004$	[12]
$\gamma$ EC	93.331	$4.51 \pm 0.16$	[11]
$\gamma\beta^-$	103.6	$0.81 \pm 0.24$	[11]

tified unambiguously to result from the  $^{180}\text{Ta}^g$  decay. Though other coincidences, e.g.,  $(\gamma, K_\beta)$  pairs, were too weak to be observed, any misinterpretation can certainly be excluded.

## 2. Data Analysis

The number of activated  $^{180}\text{Ta}^g$  nuclei is given by

$$N^{180g} = \frac{C_{\gamma, K_\alpha}}{I_\gamma P_K I_{K_\alpha} f_m f_w \epsilon A_{\gamma, K_\alpha}} C_P C_{\text{sum}} \quad (1)$$

with  $C_{\gamma, K_\alpha}$  being the number of  $(\gamma, K_\alpha)$  coincidences,  $I_\gamma$  the absolute decay intensity of the 93.3 keV  $\gamma$  transition (Table I),  $P_K = 0.809(7)$  the capture probability for  $K$ -shell electrons [11], and  $I_{K_\alpha} = 0.744(12)$  the  $K_\alpha$ -emission probability [12]. The time factors  $f_i$  denote the corrections for the decay during the measurement ( $f_m = \text{LT}/\text{RT}[1 - e^{-\lambda \text{RT}}]$ , where LT, RT are life and real time, and  $\lambda$  the decay constant of  $^{180}\text{Ta}^g$ ) as well as during the waiting time between the end of irradiation and the start of counting ( $f_w = e^{-\lambda t_w}$ ). The remaining quantities are the efficiency  $\epsilon$  for  $(\gamma, K_\alpha)$  coincidences, the correction factor  $A_{\gamma, K_\alpha}$  for photon absorption in the tantalum foil, the pile-up correction  $C_P = C_P^\gamma \cdot C_P^{K_\alpha}$  for  $\gamma$  and  $K_\alpha$  x rays, and the summing corrections  $C_{\text{sum}}$  for the respective cascades.

The correction for self-absorption is given by

$$A_{\gamma, K_\alpha} = \int n(x) e^{-\mu_{\text{eff}}(E_\gamma)(d-x)} e^{-\mu_{\text{eff}}(E_{K_\alpha})x} dx, \quad (2)$$

where  $d$  is the foil thickness,  $x$  the distance perpendicular to the surface of the foil,  $n(x)$  the statistical weight for photons originating from a layer at  $(x, x+dx)$ , and  $\mu_{\text{eff}} = k\mu_\perp$  the effective absorption coefficient for isotropic photon emission. Depending on foil thickness and photon energy, the experimental enhancement  $k = 1.45 - 1.60$  resulted in correction factors  $A_{\gamma, K_\alpha} = 0.5 - 0.6$ . Since  $\mu(E_{K_\alpha}) \neq \mu(E_\gamma)$ ,  $A_{\gamma, K_\alpha}$  and  $A_{K_\alpha, \gamma}$  were not equal either and had to be considered independently.

The pile-up correction was based on  $\gamma$  lines of induced activities which were monitored throughout the activations.

The summing correction could be neglected because the  $L$  x rays were strongly absorbed in the tantalum foils.

The results are given in terms of thick target yields

$$Y = \frac{N^{180}}{N_{\alpha} f_b} = \frac{1}{N_{\alpha} f_b} \frac{1}{I_\gamma P_K I_{K_\alpha} f_m f_w \epsilon} \frac{C}{A} C_P \quad (3)$$

where  $C/A$  denotes the weighted average of  $C_{\gamma, K_\alpha}/A_{\gamma, K_\alpha}$  and  $C_{K_\alpha, \gamma}/A_{K_\alpha, \gamma}$ . The number of incident  $\alpha$  particles,  $N_\alpha$  was inferred from the integrated beam current. The correction factor  $f_b$  accounts for the decay of the activated nuclei during irradiation (for a definition see Ref. [13]).

## B. Irradiations with protons

The proton irradiations were carried out at the 3.75 MV Karlsruhe Van de Graaff accelerator with incident energies of 3.00–3.70 MeV. The energy was determined from the magnetic field of a bending magnet. Again, the bombarded tantalum foils were water cooled and mounted in a Faraday cup similar to the one used for the  $\alpha$ -particle irradiations. Accordingly, the beam current, which was limited in this irradiation to  $\sim 50$   $\mu\text{A}$ , was digitized with a current integrator and stored in time intervals of one minute.

The detection of the induced  $^{180}\text{Ta}^g$  activity was carried out in complete analogy to the measurements described in the last paragraph because large background activities, especially  $^{18}\text{F}$  and  $^{67}\text{Ga}$ , had to be suppressed. Since the 5% HPGe detector was not available, a larger 30% HPGe detector had to be used giving rise to slightly more Compton background. The efficiency for  $(\gamma, K_\alpha)$  coincidences was measured to  $\epsilon = 10.8(5)\%$ .

## III. RESULTS

The results of the irradiations are given in terms of thick target yields and are summarized in Table II together with the characteristics of the respective irradiations. Although the background could be reduced to 5–10  $\text{h}^{-1}$ , no signal was observed when the tantalum foils were bombarded with protons. Also, the  $\alpha$ -irradiations with  $E_\alpha \geq 16$  MeV did not yield a detectable  $^{180}\text{Ta}^g$  activity due to an exponentially increasing background from the  $^{181}\text{Ta}(\alpha, n)^{184}\text{Re}$  reaction. To keep the total count rate and the pile-up effect at a tolerable level, the irradiation time had to be reduced, thus diminishing the sensitivity of the measurements greatly.

All upper limits in Table II are given in terms of a 90% confidence level [14] which reflects the detection limit of an actual signal. The systematic uncertainties of the limits are summarized in Table III; they are largest for the  $\gamma$  efficiency and for the self-absorption and pile-up corrections. The larger pile-up uncertainties refer to irradiations at the highest  $\alpha$  energies, where sizable count rates were obtained. For protons, the pile-up correction was negligible. The relatively large uncertainties for self-absorption and  $\gamma$  efficiency originate from the close counting geometry since even small displacements of the sample produce large effects. The statistical uncertainty refers to the obtained signals and dominates the total uncertainty in all cases, particularly for the irradiations at low energies. All other uncertainties are of minor importance.

TABLE II. Characteristics of the irradiations and measured yields.

Projectiles	Energy [MeV]	Irradiation time [h]	Average current [ $\mu\text{A}$ ]	Thickness Ta foil [ $\mu\text{m}$ ]	Yield [ $10^{-13}$ ]
$\alpha$ particles	12.03	6.80	14.3	47	$1.14 \pm 0.35$
	13.00	9.82	14.3	72	$2.67 \pm 1.49$
	13.86	5.58	12.8	59	$2.06 \pm 0.53$
	13.89	10.86	14.0	60	$4.66 \pm 0.91$
	14.90	9.70	15.3	61	$9.87 \pm 1.86$
	15.45	5.63	13.6	47	$9.01 \pm 2.52$
	16.05	4.08	8.4	70	$< 27.4 \pm 4.3$ (syst)
	17.03	1.38	9.8	70	$< 34.2 \pm 5.1$ (syst)
	18.00	0.50	13.8	91	$< 44.4 \pm 5.9$ (syst)
	20.08	0.20	14.1	91	$< 224 \pm 26$ (syst)
protons	3.70	15.42	50.1	46	$< (6.03 \pm 0.51) \times 10^{-2}$ (syst)

IV. DISCUSSION

A. Light ions

The coincident photon detection in these experiments allowed for the clear identification of the  $^{180}\text{Ta}^g$  decay. Since strong background reactions on impurities in the Ta foils were observed, nuclear reactions leading to  $^{180}\text{Ta}^g$  can *a priori* not be excluded. However, the number of energetically possible reactions is small, and only four reactions may produce a  $^{180}\text{Ta}^g$  signal, namely,  $^{176}\text{Lu}(\alpha, \gamma)$ ,  $^{177}\text{Hf}(\alpha, p)$ ,  $^{180}\text{Ta}(\alpha, \alpha')$ , and  $^{181}\text{Ta}(\alpha, \alpha'n)$ . The reactions on the lutetium and hafnium impurities can be excluded because of their small abundances. At low bombarding energies where the  $^{180}\text{Ta}^g$  activity was observed, nuclear inelastic scattering on  $^{180}\text{Ta}$  can also be neglected [15].

The excitation function for the formation of the compound nucleus of the  $^{181}\text{Ta}(\alpha, \alpha'n)$  reaction was calculated with the optical model [16], and is plotted in Fig. 4 (dotted curve). The measured data as well as the  $E_2$ -,  $E_3$ -Coulomb excitation functions for IS at 2.0, 1.5, and 0.5 MeV are also shown in this figure. All excitation functions are normalized

arbitrarily to the data at 13.9 MeV. Since the nuclear excitation function is much steeper, the compound nucleus reaction can certainly be ruled out. Direct contributions to the  $(\alpha, \alpha'n)$  reactions were estimated with the coupled channels code ECIS94 by assuming excitation of the giant dipole and quadrupole resonances and subsequent decay by neutron emission. For the relevant incident energies these contributions can also be neglected [15]. Thus, the only mechanism responsible for the observed  $^{180}\text{Ta}^g$  activity is Coulomb excitation.

The Coulomb excitation functions are calculated from

$$Y_{E\lambda} = N_{\text{target}} \int \frac{\sigma_{E\lambda}(E)}{dE/dx(E)} dE \quad (4)$$

with  $N_{\text{target}}$  denoting the number of target nuclei,  $dE/dx(E)$  the stopping power for the incident ions [17], and  $\sigma_{E\lambda}$  the Coulomb excitation cross section for a transition of type  $E\lambda$ . A numerical evaluation of the latter can be found in Alder *et al.* [18], where  $E1$ ,  $E2$  cross sections are calculated quan-

TABLE III. Compilation of uncertainties.

Type and source of uncertainty	Quantity	Uncertainty (%)		
Systematical	Irradiation	$E_\alpha$	0.3	
		$E_p$	0.5	
		$N_\alpha$	1.5–3.6	
		$N_p$	<1.0	
		$f_b$	<0.1	
	Literature Data	$I_\gamma$	3.5	
		$I_{K_\alpha}$	1.6	
		$P_K$	0.9	
		Measurement	$C_p$	4.5–12.3
			$f_w$	0.1
	$f_m$		<0.1	
	Statistical	$A_{\gamma, K_\alpha}$	7.0	
		$\epsilon$	5.0	
$C$			12.9–55.3	

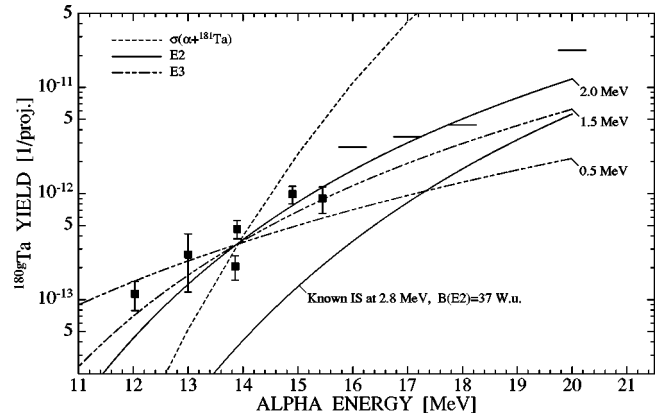


FIG. 4. Graphical representation of the results from the irradiation with  $\alpha$  particles. Included are Coulomb excitation functions to various assumed IS and the nuclear excitation function for forming the compound nucleus of the  $^{181}\text{Ta}(\alpha, n)$  reaction. This reaction can be excluded due to the much steeper increase with  $\alpha$  energy. Excitation of the known IS at 2.8 MeV must also be ruled out.

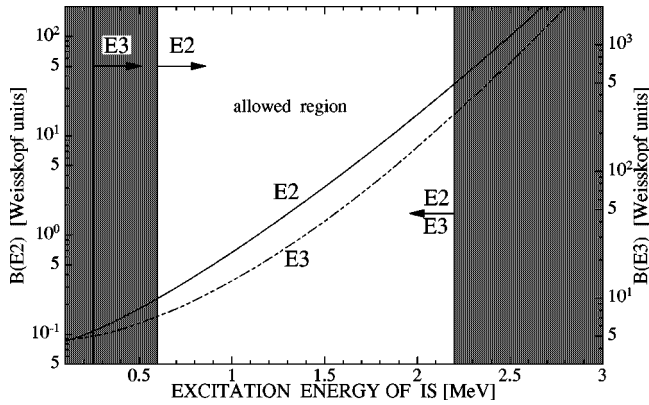


FIG. 5. Allowed excitation energy and reduced transition probability for the IS compatible with the results from the irradiations with protons and  $\alpha$  particles.

tum mechanically, and all further orders in semiclassical approximation. The uncertainties in the calculated yields, which are dominated by the uncertainties in the stopping cross sections, are typically 5% and can be neglected in view of the poor statistics of the data.

In principle, the excitation energy of the IS can be derived from the shape of the excitation function. However, since the data exhibit large statistical uncertainties and are restricted to a small energy interval for the  $\alpha$  particles, the energy of the IS can only be estimated. An upper limit of approximately 2.2 MeV is deduced from the null results at higher bombarding energies. The best fit to the data is obtained for an IS at 1.5 MeV, almost irrespective of the assumed multipolarity ( $E2$ ,  $E3$ ) of the transition.

The Coulomb excitation function for the known IS at 2.8 MeV [6] is also included in Fig. 4. Assuming an  $E2$  transition, the integrated absorption cross section of this IS was converted into a reduced transition probability of  $B(E2) = 37$  Weisskopf units. Clearly, this value is far too small to fit the experimental data, the  $\alpha$  particles being too insensitive for exciting such high-lying levels. This holds for other multipolarities ( $M1, E1$ ) as well.

How do the upper limits obtained in the proton irradiations compare to the results of the  $\alpha$  bombardments? If the Coulomb excitation probability of both particles is considered, the sensitivity of the protons increases more strongly with decreasing excitation energy. Therefore, the missing signal in the proton irradiation allows us to set a lower limit for the excitation energy of the IS. Since the excitation probability is the larger the lower the multipolarity of the transition, the most stringent limit is found for the lowest multipolarity.

Figure 5 summarizes the results of both experiments in terms of an allowed range for the excitation energy of the IS: 0.6–2.2 MeV or 0.25–2.2 MeV, if  $E2$ , or  $E3$  transitions are assumed, respectively. The corresponding  $B(E\lambda)$  values are given on the y axis. Higher multipole orders or magnetic excitation can be excluded since these assumptions would require unrealistically large reduced transition probabilities. Furthermore,  $E1$  is ruled out by the null result from the bremsstrahlung irradiations of Collins *et al.* [6] [ $\sigma\Gamma(E_{\text{ex}} \approx 1.4 \text{ MeV}) < 5 \times 10^{-27} \text{ cm}^2 \text{ keV}$ ]. For an  $E2$  transition, this upper limit restricts also the allowed range of the IS to lower

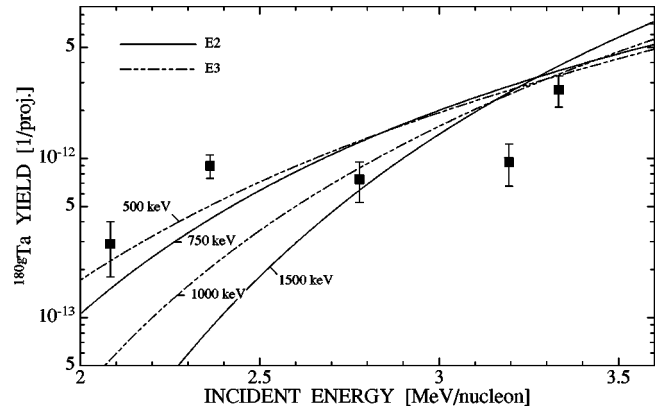


FIG. 6. Calculated Coulomb excitation functions for  $^{36}\text{S}$  to IS compatible with the results of the  $\alpha$  irradiations (see Fig. 5) in comparison to the low-energy results of Ref. [9] (solid squares). Despite the scatter of the data, the overall agreement suggests that the  $^{36}\text{S}$  yields at low energies are at least partly due to Coulomb excitation.

excitation energies. A level at 2.2 MeV can be excluded but an IS at 1.5 MeV would still be compatible. Other limits from experiments using primary  $\gamma$  sources such as  $^{60}\text{Co}$  and  $^{137}\text{Cs}$  [5,19] are not sensitive enough to provide further limitations.

Large reduced transition probabilities are needed to fit the data, especially if an  $E3$ -transition is assumed. This holds the more since not all decay channels of the IS lead to the ground state. Accordingly, the reduced transition probabilities in Fig. 5 are lower limits of the actual  $B(E\lambda)$  values for the transition from the isomer to the IS. In this regard an  $E2$  transition seems to be more likely. But as a consequence, only few angular momentum can be transferred and the transition has to proceed through a  $K$  cascade. Because of the limited number of levels at low energies, the IS is then situated at rather high excitation energy as suggested by the best fit to the present data.

## B. Heavy ions

New Coulomb excitation measurements have been performed with oxygen ions [10] and with  $^{36}\text{S}$  ions [20]. The latter results confirmed the previously obtained behavior of the excitation function. However, when the measurements were repeated with an enriched  $^{180}\text{Ta}$  target, the yields did not show the expected correlation with the  $^{180}\text{Ta}$  abundance. Whether this implies another mechanism for producing a significant part of the Coulomb excitation yields measured with the natural tantalum target is currently investigated by a comparison with the absolute yields from a corresponding natural target. Nevertheless, the overall concurrence with the results of the  $\alpha$  irradiations shown in Fig. 6 indicates that the data must be, at least partly, due to Coulomb excitation. However, the sulfur data at low energies suggest the IS at fairly low excitation energy ( $< 750 \text{ keV}$ ), in contrast to the results of the  $\alpha$  irradiations, which yield a best fit for  $E_{\text{ex}} \sim 1.5 \text{ MeV}$ .

## C. $^{184}\text{Re}$ yields

As mentioned before, the detection of the  $^{180}\text{Ta}^g$  decay after irradiation with  $\alpha$  particles was hampered by the strong

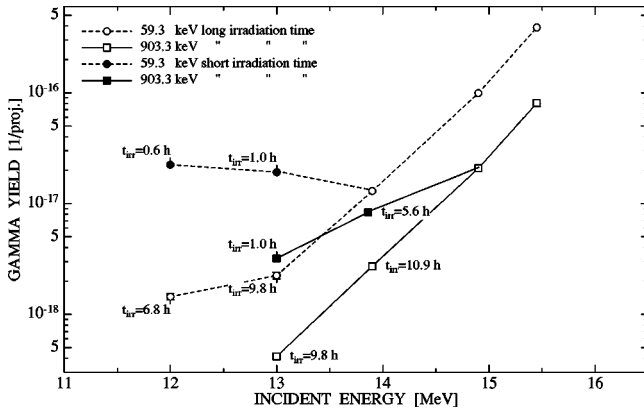


FIG. 7. The  $\gamma$  yield from the decay of  $^{184}\text{Re}$  after the irradiations with  $\alpha$  particles. The respective uncertainties are smaller than the size of the symbols. The obvious discrepancies with respect to different irradiation times indicate a yet unknown isomer with a half-life of approximately 2 h.

background activity. The dominant contribution came from the EC decay of  $^{184}\text{Re}$  ( $t_{1/2} = 38.0\text{d}$ ) that was produced via  $(\alpha, n)$  reactions on the abundant  $^{181}\text{Ta}$ . Surprisingly, the observed  $^{184}\text{Re}$  yields showed large discrepancies for different irradiation times. This situation is illustrated in Fig. 7 for the associated  $K_{\alpha 2}$  x rays at 59.3 keV and the 903.3 keV  $\gamma$  rays from the decay of  $^{184}\text{Re}^g$ . Repeated activations with different irradiation times at  $E_\alpha = 12.0, 13.0, 13.9$  MeV were found to produce incompatible yields, the respective discrepancies becoming larger with decreasing irradiation times. Loss of activity, e.g., by absorption or sputtering, was excluded by analyzing the yields of several induced background activities, especially at  $E_\alpha = 12.0$  MeV where the same target foil was used in two different activations. In fact, the discrepancies were found only for the  $^{184}\text{Re}$  yields. The identification of the  $^{184}\text{Re}^g$  was supported by the coincidence spectra where the deviations with respect to irradiation times appeared as well. Since other decays contributing to the  $\gamma$  rays in Fig. 7 can be ruled out, the observed effect suggests the existence of a new isomer in  $^{184}\text{Re}$ , for which a half-life of about 2 h was estimated from a fit of the observed intensities.

V. ASTROPHYSICAL IMPLICATIONS

The depopulation of the stable isomer via transitions to the IS can be expressed through an effective half-life for the isomer. Obviously, the strength of the coupling will be very sensitive to the population probability of the IS, i.e., to the temperature in the stellar environment. In Fig. 8, the effective half-life of the  $9^-$  isomer is plotted as a function of temperature for IS at 0.6 and 1.5 MeV excitation energy and with  $B(E\lambda)$  values compatible to the results from the irradiations with  $\alpha$  particles. The curves were calculated by solving the coupled differential equations of the three level system (isomer  $\leftrightarrow$  IS  $\leftrightarrow$  ground state) including the time for reaching thermal equilibrium. Compared to previous evaluations, this yields longer half-lives, especially for higher lying IS (for a more detailed evaluation see Refs. [13,21]). The retardation of the EC-decay of the ground state due to the almost complete ionization was neglected since this effect has little impact on the effective half-life in the relevant temperature window of the  $s$  process.

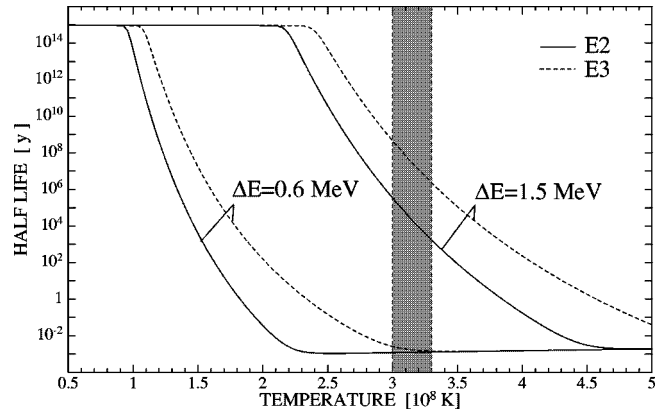


FIG. 8. Effective half-life of  $^{180}\text{Ta}^m$  versus temperature for intermediate states at 0.6 and 1.5 MeV excitation energy. The shaded band corresponds to the most plausible temperature range for the  $s$ -process production of  $^{180}\text{Ta}$  (see text).

At the various stellar sites which were considered for an  $s$ -process origin of  $^{180}\text{Ta}$  [5] this isotope is synthesized predominantly through neutron captures on its radioactive progenitor  $^{179}\text{Ta}$ . During the carbon shell burning phase at the end of stellar evolution in massive stars ( $> 25M_\odot$ ), the prevailing temperatures of about 1 GK are high enough for an efficient coupling of isomer and ground state via the already known IS at 2.8 MeV [22,23]. Accordingly, all synthesized  $^{180}\text{Ta}$  nuclei are destroyed. This holds also for the nucleosynthesis in carbon core burning of stars with 15 and 30 solar masses [24]. In contrast, helium shell burning in low mass AGB stars, where the majority of the  $s$  isotopes is synthesized (main  $s$ -process component) seems to be a more promising production site for  $^{180}\text{Ta}$ . In this scenario, the  $s$  process occurs in a thin helium shell which burns in repeated flashes for a time span of 200–300 years with interpulse phases of approximately 50 000 years [25]. During He burning,  $^{180}\text{Ta}$  is synthesized within a rather short period of a few years when the  $^{22}\text{Ne}(\alpha, n)^{25}\text{Mg}$  neutron source is activated at temperatures of 250 to 300 MK.

The temperature window for a significant  $s$ -process synthesis is indicated in Fig. 8. At temperatures below 300 MK, the branching in the  $s$ -process path at  $^{179}\text{Hf}$  is not sufficiently developed. Consequently, too few  $^{179}\text{Ta}$  nuclei are available for further neutron capture synthesis. At temperatures above 330 MK, however, the  $s$  contribution to the  $p$ -process nucleus  $^{180}\text{W}$  is exceeding a tolerable limit of  $\sim 30\%$ . Since the proper temperature conditions exist only for a comparably short time, an IS around 1.5 MeV would not impede the production of  $^{180}\text{Ta}$ . However, if the IS is situated below 1.2 MeV, examination of the time-dependent reaction flow shows that only  $\sim 25\%$  of the solar system abundance of  $^{180}\text{Ta}$  can be produced in this scenario, since the temperatures in this particular  $s$ -process model are hardly exceeding 300 MK [25]. Together with the  $s$  contribution from the branching in  $^{180}\text{Hf}$  approximately half of the solar system abundance could then be explained in this way.

What are the mechanisms that might account for the missing half? A possible nuclear physics uncertainty is the population probability of the isomeric state in stellar neutron captures, which has not been measured so far. Theoretical calculations of the branching ratio with the statistical model

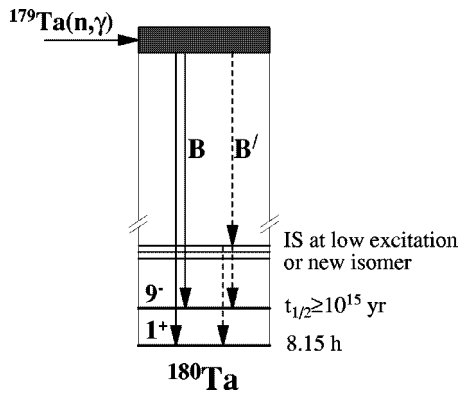


FIG. 9. Population of the stable isomer  $^{180}\text{Ta}^m$  in the  $s$  process. The branching ratio  $B$  is sensitive to IS at low excitation energy as well as to additional isomers which might be populated in neutron capture reactions (dotted arrows).

[5] did not include large  $K$  mixing at low excitation energy. Since the spins of the cascading states are the determining quantity for the branching ratio, the population of states with large  $K$  mixing, such as the IS, will certainly influence the branching ratio. Therefore, an enhanced feeding of the stable isomer may well be possible (see Fig. 9). This argument applies also if there are yet unknown isomers in  $^{180}\text{Ta}$ , a plausible possibility in view of the large spin difference between the  $9^-$  isomer and the  $1^+$  ground state. On the other hand, uncertainties of the stellar model have to be considered as well. The calculations of Gallino *et al.* [25] are based on a star with solar metallicity. Stars with lower metallicities exhibit higher temperatures and higher neutron fluxes, thus favoring the production of  $^{180}\text{Ta}$ .

Aside from the possibility of an enhanced  $s$ -process production, there are alternative mechanisms to account for the synthesis of the remaining half or even for all of the  $^{180}\text{Ta}$ . In these scenarios, the existence of an IS has negligible influence on the synthesis of  $^{180}\text{Ta}$ , either due to the low temperatures [1,2] or to the very short time scales [3,4].

From a discussion of explosive nucleosynthesis scenarios, any sizable  $r$ -process contributions from the direct isomer to isomer decay of  $^{180}\text{Hf}^m$  can be neglected [26]. Prantzos *et al.* [4] showed that the  $p$  process in supernovae of type II could be a promising site. However, considering that the major part of the  $p$  nuclei may be synthesized in supernovae of type Ia, the overproduction factor of Prantzos *et al.* might be too small to account for all of the  $^{180}\text{Ta}$  abundance.

Spallation reactions in the interstellar medium [1] seem to be a rather speculative possibility, since it requires the existence of an enhanced low energetic component in the cosmic ray flux. Originally, this component was introduced to explain the abundances of  $^7\text{Li}$  and  $^{11}\text{B}$ , but meanwhile the  $\nu$  process (see below) seems to account for these abundances. Apart from the existence of an enhanced low energetic cosmic ray flux, the uncertainties in the assumed production cross sections, in the abundance pattern of the cosmic ray flux, and in the branching ratio for the population of the stable isomer are further obstacles for a quantitative discussion of this mechanism.

The synthesis of  $^{180}\text{Ta}$  by photodisintegration of  $^{181}\text{Ta}$  during hydrostatic H burning [2] appears to offer another speculative explanation, since these calculations did not in-

clude the destruction reaction  $^{180}\text{Ta}(\gamma, n)$ , nor did they consider the partial population of the stable isomer. Although a coupling of isomer and ground state can be neglected due to the low temperatures, it is not clear what fraction of the synthesized  $^{180}\text{Ta}$  nuclei would be exposed to the consecutive burning stages at higher temperatures. Furthermore, the amount of  $^{180}\text{Ta}$  that can be returned from these zones into the interstellar medium remains an open question.

A promising alternative to an  $s$ - or  $p$ -process origin is the synthesis of  $^{180}\text{Ta}$  in the  $\nu$  process via  $^{181}\text{Ta}(\nu, \nu'n)$  reactions induced by the intense neutrino flux ejected from the collapsing core in supernovae of type II [3]. Despite of the remaining uncertainties, the  $\nu$  process represents certainly a serious mechanism for the production of  $^{180}\text{Ta}$ .

## VI. CONCLUSIONS

The existence of an intermediate state located below 2.2 MeV excitation energy was confirmed by Coulomb excitation of  $^{180}\text{Ta}$  using  $\alpha$  particles. The transition from the stable isomer to the IS was determined to be either  $E2$  or  $E3$ .

Since the excitation energy of the IS could also not be determined accurately in the present study, the survival of the  $^{180}\text{Ta}$  nuclei at  $s$  process temperatures remains an open question. The best fit to the data is obtained for an IS at 1.5 MeV which would allow for an efficient  $s$  process production of  $^{180}\text{Ta}$ .

To quantify the  $s$  process production of  $^{180}\text{Ta}$  more thoroughly, further improvements of the nuclear physics data are definitely required. A repetition of the experiments with light ions using an enriched metallic  $^{180}\text{Ta}$  sample would allow us to improve the statistics and to determine the shape of the excitation function more precisely. Additional constraints for the excitation energy of the IS are expected from a recent repetition of the Coulomb excitation experiment with sulfur ions [9] using an enriched  $^{180}\text{Ta}$  sample [20]. Furthermore, an irradiation of an enriched  $^{180}\text{Ta}$  sample in an intense bremsstrahlung spectrum is currently under way [27] which will be sensitive enough to observe an  $E2$  transition. Aside from the destruction of  $^{180}\text{Ta}$  in the stellar medium, the  $s$  process production factors are uncertain as well. This follows from the existence of the large  $K$  mixing at low excitation energies influencing the  $\gamma$  cascades to the stable isomer. Current efforts to measure the neutron capture cross section of  $^{179}\text{Ta}$  will hopefully solve this problem in the near future [28].

## ACKNOWLEDGMENTS

We would like to thank the operating teams of the PTB cyclotron (O. Döhr, H. Eggstein, M. Hoffmann, M. Karalus) and of the Karlsruhe Van de Graaff accelerator (E. Knaetsch, D. Roller, W. Seith) for providing us with excellent beam conditions as well as G. Rupp for his tireless technical support. We are grateful to J. Kiener and A. Mengoni for their theoretical calculations of the  $^{180}\text{Ta}(\alpha, \alpha')$  and  $^{181}\text{Ta}(\alpha, an)$  cross sections, and to J. de Boer, M. Loewe, P. von Neumann-Cosel, and E. Norman for stimulating and critical discussions.

- [1] K. Hainebach, D. Schramm, and J. Blake, *Astrophys. J.* **205**, 920 (1976).
- [2] T. Harrison, *Astrophys. Lett.* **17**, 61 (1976).
- [3] S. Woosley, D. Hartmann, R. Hoffman, and W. Haxton, *Astrophys. J.* **356**, 272 (1990).
- [4] N. Prantzos, M. Hashimoto, M. Rayet, and M. Arnould, *Astron. Astrophys.* **238**, 455 (1990).
- [5] Z. Németh, F. Käppeler, and G. Reffo, *Astrophys. J.* **392**, 277 (1992).
- [6] C. Collins *et al.*, *Phys. Rev. C* **42**, 1813 (1991).
- [7] S. Drissi (private communication).
- [8] E. Norman (private communication).
- [9] C. Schlegel, P. von Neumann-Cosel, F. Neumeyer, A. Richter, and S. Strauch, *Phys. Rev. C* **50**, 2198 (1994).
- [10] Y. Chan, R. Larimer, M. Moorhead, E. Norman, M. Perillo-Isaac, S. Bayer, E. Bezakova, and A. Byrne (in preparation).
- [11] ENDF File, National Nuclear Data Center, Brookhaven National Laboratory.
- [12] E. Browne and R. Firestone, *Table of Radioactive Isotopes* (Wiley, New York, 1986).
- [13] M. Schumann, Report No. FZKA-5985, Forschungszentrum Karlsruhe, 1997.
- [14] O. Helene, *Numer. Math.* **212**, 319 (1983).
- [15] J. Kiener (private communication).
- [16] A. Mengoni (private communication).
- [17] J. Ziegler, *Handbook of Stopping Cross-Sections for Energetic Ions in all Elements* (Pergamon Press, New York, 1980), Vol. 5.
- [18] K. Alder, A. Bohr, T. Huus, B. Mottelson, and A. Winther, *Rev. Mod. Phys.* **28**, 432 (1956).
- [19] E. Norman, S. Kellogg, T. Bertram, S. Gil, and P. Wong, *Astrophys. J.* **281**, 360 (1984).
- [20] M. Loewe (private communication).
- [21] C. Theis, Ph.D. thesis, University of Heidelberg, 1995.
- [22] C. Raiteri, M. Busso, R. Gallino, G. Picchio, and G. Pulone, *Astrophys. J.* **367**, 228 (1991).
- [23] C. Raiteri, M. Busso, R. Gallino, and G. Picchio, *Astrophys. J.* **371**, 665 (1991).
- [24] J. Arcoragi, N. Langer, and M. Arnould, *Astron. Astrophys.* **249**, 134 (1991).
- [25] R. Gallino, C. Arlandini, M. Busso, M. Lugaro, C. Travaglio, O. Straniero, A. Chieffi, and M. Limongi, *Astrophys. J.* **497**, 388 (1998).
- [26] S. Kellogg and E. Norman, *Phys. Rev. C* **46**, 1115 (1992).
- [27] H. Pitz *et al.* (private communication).
- [28] C. Arlandini, M. Schumann, and F. Käppeler (in preparation).